Stacking order dependence of inverse spin Hall effect and anomalous Hall effect in spin pumping experiments

Sang-Il Kim, Dong-Jun Kim, Min-Su Seo, Byong-Guk Park, and Seung-Young Park

Citation: Journal of Applied Physics **117**, 17D901 (2015); doi: 10.1063/1.4906176
View online: http://dx.doi.org/10.1063/1.4906176
View Table of Contents: http://scitation.aip.org/content/aip/journal/jap/117/17?ver=pdfcov
Published by the AIP Publishing

Stacking order dependence of inverse spin Hall effect and anomalous Hall effect in spin pumping experiments

Sang-Il Kim,[1] Dong-Jun Kim,[2] Min-Su Seo,[1] Byong-Guk Park,[2] and Seung-Young Park[1,a)]
[1]*Division of Materials Science, Korea Basic Science Institute, Daejeon 305-806, South Korea*
[2]*Department of Materials Science and Engineering, KAIST, Daejeon 305-701, South Korea*

(Presented 7 November 2014; received 1 September 2014; accepted 20 September 2014; published online 15 January 2015)

The dependence of the measured DC voltage on the non-magnetic material (NM) in NM/CoFeB and CoFeB/NM bilayers is studied under ferromagnetic resonance conditions in a TE_{011} resonant cavity. The directional change of the inverse spin Hall effect (ISHE) voltage V_{ISHE} for the stacking order of the bilayer can separate the pure V_{ISHE} and the anomalous Hall effect (AHE) voltage V_{AHE} utilizing the method of addition and subtraction. The Ta and Ti NMs show a broad deviation of the spin Hall angle θ_{ISH}, which originates from the AHE in accordance with the high resistivity of NMs. However, the Pt and Pd NMs show that the kinds of NMs with low resistivity are consistent with the previously reported θ_{ISH} values. Therefore, the characteristics that NM should simultaneously satisfy to obtain a reasonable V_{ISHE} value in bilayer systems are large θ_{ISH} and low resistivity.
 [http://dx.doi.org/10.1063/1.4906176]

I. INTRODUCTION

The injection of pure spin current J_s into adjacent non-magnetic materials (NMs) has demonstrated strong potential for the development of applied spintronic devices.[1] The J_s injection processes are commonly elucidated using three general methods such as thermal spin injection,[2] electrical spin injection,[3] and ferromagnetic resonance (FMR).[4,5] In particular, spin pumping, which is the generation of J_s from FMR, in a NM/ferromagnet (FM) bilayer enables efficient spin injection into metals and semiconductors free from the impedance mismatch problem.[6] The inverse spin Hall effect (ISHE) in the NM/FM bilayers is commonly used for detecting J_s generated by precessing magnetization M. This injected J_s is converted into an ISHE current J_{ISHE} via the ISHE as[4]

$$J_{ISHE} = \theta_{ISH}\left(\frac{2e}{\hbar}\right)J_s \times \sigma, \tag{1}$$

where θ_{ISH}, e, $\hbar$, and σ denote the spin Hall angle, elementary charge, Dirac constant, and spin-polarization vector of J_s, respectively. Here, θ_{ISH} represents the efficiency of the spin-charge conversion in NM, which is measured for several metals and alloys.[7–9] It is well known that θ_{ISH} can be obtained from the experimental ISHE voltage V_{ISHE} signal using a phenomenological model of spin pumping.[10]

Moreover, the strength of spin-orbit coupling (SOC) contributes to the amplitude of V_{ISHE}. Generally, the interaction between spin and orbital angular momentum generates the anomalous Hall effect (AHE), ISHE, and other spin-related phenomena in magnetic systems. For example, in the resonant cavity, the in-plane component of a microwave electric field E_{MW} in the FM layer may induce an AHE current J_{AHE} via the AHE in conjunction with FMR. Then, J_{AHE} can be expressed as[11]

$$J_{AHE} \propto E_{MW} \times m, \tag{2}$$

where m is the M component perpendicular to E_{MW}. As a result, V_{ISHE} at the NM layer should overlap with the AHE voltage V_{AHE} at the FM layer due to originating SOC in the NM/FM bilayer systems. Therefore, the values of θ_{ISH} estimated to V_{ISHE} largely vary in accordance with the ratio of $V_{AHE}/(V_{ISHE}+V_{AHE})$, which is consistent with a simple circuit model for the FM/NM bilayer.[11]

Thus, far, to attain more accurate θ_{ISH}, many studies have been decreased the AHE terms. When the V_{ISHE} measurement is performed, the bilayer sample was placed at the center of a resonant cavity where the magnetic field was maximized, while E_{MW} was minimized, which in turn minimizes the AHE.[12] On the other hand, the selection of microwave modes is important despite the optimized centering.[13] The AHE contribution of the TE_{011} mode is larger than that of the TE_{102} mode. In case of the TE_{011} mode, the bilayer sample is easily exposed to E_{MW} in all directions. However, these previous results remain unclear on the origin or correlation of the ISHE and AHE in bilayer structures.

In this paper, the dependence of NMs on measuring the DC voltage V under FMR conditions is experimentally investigated to examine the CoFeB/*NM* and *NM*/CoFeB bilayers, where *NM* = Pt, Pd, Ta, and Ti. The sign of the directional V_{ISHE} depends on the stacking order of layers between CoFeB and *NM*, which are designed as CoFeB/*NM* or *NM*/CoFeB. However, the V_{AHE} sign is not associated with the order of the layer. Therefore, the pure V_{ISHE} and V_{AHE} can be separated utilizing the method of addition and subtraction in the bilayer structure. Then, the estimated θ_{ISH} from the pure V_{ISHE} is compared with the reported values for different NMs. Both Ta and Ti materials show a broad deviation in θ_{ISH}, which originates from the enormous AHE in

a)Author to whom correspondence should be addressed. Electronic mail: parksy@kbsi.re.kr.

accordance with the high resistivity of NMs. Therefore, the NM characteristics should be simultaneously satisfied with large θ_{ISH} and low resistivity to obtain reasonable and pure V_{ISHE} values in a bilayer system.

II. EXPERIMENT

Figures 1(a) and 1(b) show schematic illustrations of the CoFeB/*NM* and *NM*/CoFeB (*NM* = Pt, Pd, Ta, and Ti) bilayers used in these experiments, respectively. The samples are bilayer systems comprised of a 10-nm-thick ferromagnetic CoFeB layer and a 10-nm-thick *NM* layer sputtered on thermally oxidized Si substrates. All bilayer samples have a size of 1 mm (width) × 2 mm (length). Two electrodes are connected to the ends of the sample. The present experiments minimized the effect of E_{MW} by optimizing the device under test (DUT) centering by placing the DUT near the center of a TE_{011} cylindrical cavity. The external magnetic field H is applied perpendicular to the direction across the electrodes. Figure 1(a) shows that V measured for the CoFeB/NM bilayer is described using Eqs. (1) and (2) as

$$V_{CoFeB/NM} = V_{ISHE}(//J_s \times \sigma) + V_{AHE}(//E_{MW} \times m). \quad (3)$$

On the other hand, V measured for the NM/CoFeB bilayer is also expected to be

$$V_{NM/CoFeB} = -V_{ISHE}(// - J_s \times \sigma) + V_{AHE}(//E_{MW} \times m). \quad (4)$$

Ultimately, the J_s-sign governed by the directional spin pumping is changed by inverting the orders of the layers, as shown in Fig. 1(b), which looks like the bilayer sample is rotated. For example, the sign of V_{ISHE} is reversed by reversing the H or J_s-directions.[14] However, V_{ISHE} delicately contributes to the variation of the E_{MW} profile at the center of the cavity resonator. Moreover, it is difficult to separate these two effects because the sign of the effects can have the same directions, depending on the rotation of the sample. Therefore, structurally exchanging FM and NM allows us to obtain the pure V_{ISHE} and V_{AHE} without changing the microwave profile of cavity inside.

In the FMR measurements, the microwave frequency is 9.46 GHz and the power is 50 mW. The resonance field H_0 is around 857 Oe. Simultaneously, the value of V for the various NMs is measured under the FMR condition.

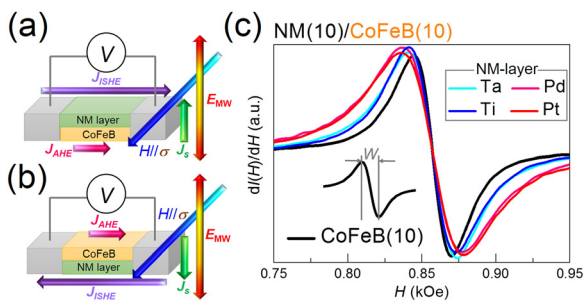

FIG. 1. (a) Schematic illustration of the bilayer sample (CoFeB/NM) used in the present study, where V_{ISHE} and V_{AHE} have the same sign. (b) Schematic illustration of the bilayer sample (*NM*/CoFeB) used in the present study. Here, V_{ISHE} and V_{AHE} have opposite signs. (c) The FMR spectra for the CoFeB single layer and *NM*/CoFeB (*NM* = Pt, Pd, Ta, and Ti) bilayer in the TE_{011} resonant cavity.

III. RESULTS AND DISCUSSION

Figure 1(c) shows the FMR spectra for the *NM*/CoFeB (*NM* = Pt, Pd, Ta, and Ti) bilayer and a CoFeB sample. Here, I denotes the microwave absorption intensity. The half width at half maximum of $I(H)$, W ($=4\pi f_0\alpha/\sqrt{3}\gamma$, shown in the inset), for the CoFeB sample is clearly enhanced by attaching the NMs layer, where f_0, α, and γ are the resonance frequency, the Gilbert damping constant, and the gyromagnetic ratio, respectively. These results experimentally demonstrate the evidence of J_s-injection due to the spin-pumping method. The value of α for the CoFeB sample is estimated to be 0.0077 from the FMR spectral width, which agrees reasonably well with the reported $\alpha = 0.015$ for a 5-nm CoFeB sample.[13] It is two times larger than that of the 10-nm CoFeB sample, which is given by $\alpha \propto 1/(\text{thickness of FM layer})$.

Figures 2(a) and 2(b) show the H dependence of V measured for the *NM*/CoFeB and CoFeB/*NM* bilayers. The measured V signals under the FMR condition are well fitted using the following function:[4,13]

$$V(H) = V_{ISHE}(H) + V_{AHE}(H) = V_{ISH}\frac{\Gamma^2}{(H-H_0)^2+\Gamma^2} + V_{AH}\frac{-2\Gamma(H-H_0)}{(H-H_0)^2+\Gamma^2}, \quad (5)$$

where the first and second terms indicate the ISHE (V_{ISH} indicates the magnitude of the first term) and AHE (V_{AH} indicates the magnitude of the second term) contributions, respectively, and Γ is the damping constant. Here, V_{ISHE} and V_{AHE} are proportional to the inverse spin Hall coefficient in NMs and the anomalous Hall coefficient in CoFeB, respectively. The signs of the V signals using the *NM* layer of Pt and Pd are distinctly reversed between the *NM*/CoFeB (Fig. 2(a)) and CoFeB/*NM* (Fig. 2(b)) bilayers. Furthermore, the spectra shapes using Pt and Pd are well reproduced using simple Lorentzian functions. These results indicate that the ISHE contribution dominates the measured V signal, which is estimated as $V_{ISH}/V_{AH} \approx 23$ (for Pt/CoFeB) and 27 (for Pd/CoFeB).

However, in case of the *NM* layer of Ta and Ti, despite the inverted layer order, the V signal shows that it is difficult to understand the reversed sign of V_{ISHE} under the primary

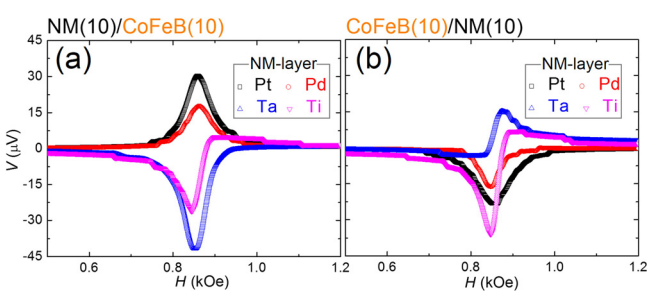

FIG. 2. The H dependence of V for (a) *NM*/CoFeB and (b) CoFeB/*NM* bilayer samples, where *NM* = Pt, Pd, Ta, and Ti.

ISHE contribution. These results indicate that the analysis of the V signal for the case of Ta and Ti-NM layer precisely consider not only the ISHE but also the AHE contribution in bilayer structures, which are estimated as $V_{ISH}/V_{AH} \approx 7$ (for Ta/CoFeB) and 1.8 (for Ti/CoFeB).

Figure 3 shows the H dependence of pure V_{ISHE} in the bilayer structures. To properly separate the pure spin-pumping contribution, the pure V_{ISHE} is described utilizing the subtraction method from Eqs. (3) and (4) as

$$V_{NM/CoFeB} - V_{CoFeB/NM} = 2V_{ISHE}(H). \tag{6}$$

Compared with previous experimental results (Fig. 2), note that the V_{ISHE} signal is well defined by the Lorentzian functions in all NMs, which excludes the AHE contribution from the measured V signals. In particular, the Ta and Ti-NMs cases can be used to consider only the ISHE contribution in spite of the large AHE. The bilayer structure utilizing the Ta-NM show the opposite sign of θ_{ISH} compared to the other NMs.

Here, V_{ISH} is designated as the peak height of the Lorentzian function in the V_{ISHE} spectrum (see Fig. 3). For the bilayer systems, V_{ISH} is given by[15]

$$V_{ISH} \approx \lambda_{NM}\tanh\left(\frac{d_{NM}}{2\lambda_{NM}}\right)\left(\frac{R_{NM}R_{CoFeB}}{R_{NM}+R_{CoFeB}}\right) \times \theta_{ISH}\left(W_{NM/CoFeB} - W_{CoFeB}\right), \tag{7}$$

where λ_{NM} is the spin diffusion length in NM, d_{NM} is the thickness of NM, R_{NM} is the resistance of NM layer, R_{CoFeB} is the resistance of CoFeB layer, $W_{NM/CoFeB}$ is the FMR spectral width of NM/CoFeB bilayer, and W_{CoFeB} is the FMR spectral width of CoFeB layer, respectively. The inset in Fig. 3 shows the R_{NM} for Pt, Pd, Ta, and Ti and R_{CoFeB}, which is measured for a single layer. To obtain θ_{ISH} for various NMs, we used Eq. (7) with the parameters $\lambda_{NM} = 10$ nm (Pt), 9 nm (Pd), 1.8 nm (Ta), and 300 nm (Ti), the difference between $W_{NM/CoFeB}$ and W_{CoFeB} (see Fig. 1(c)), and the V_{ISH} values. We obtained θ_{ISH} of Pt, Pd, Ta, and Ti as $\theta_{ISH} = 0.03$ (Pt), 0.01 (Pd), −0.02 (Ta), and 0.0021 (Ti), respectively, which are consistent with the literature values.[7–9] Finally, the bilayer samples with the Ta and Ti-NM layer (related to large AHE) exhibit different V_{ISH} values ($V_{ISH} = -42\,\mu$V (or 11.2 μV) for Ta/CoFeB (or CoFeB/Ta); $V_{ISH} = -20\,\mu$V (or −29.1 μV) for Ti/CoFeB (or CoFeB/Ti)) according to the order of the layers (see Figs. 2(a) and 2(b)), the E_{MW} profile of the cavity inside, possibility of oxidation problem depending on an air exposure, and so on, which may result in controversial and deviated θ_{ISH} values. On the other hand, the bilayer samples with the Pt and Pd-NM layer (related to little AHE) show almost same V_{ISH} values ($V_{ISH} = 30\,\mu$V (or $-28\,\mu$V) for Pt/CoFeB (or CoFeB/Pt); $V_{ISH} = 17.6\,\mu$V (or $-16.6\,\mu$V) for Pd/CoFeB (or CoFeB/Pd)) despite changing the order of the layers.

Figure 4 shows the H dependence of pure V_{AHE} in the bilayer structures. Against the aforementioned analysis, the pure V_{AHE} utilizing the addition method is described using Eqs. (3) and (4) as

$$V_{NM/CoFeB} + V_{CoFeB/NM} = 2V_{AHE}(H). \tag{8}$$

The shape of the pure V_{AHE} spectra is consistent with the above-mentioned prediction. Here, V_{AH} is designated as half of the peak-to-peak height of the V_{AHE} spectrum. The V_{AH} values of the Pt and Pd NM cases are also smaller than that of the Ta and Ti cases in the NM/FM bilayers. To analyze the contribution of AHE in the bilayers, we assume that the NM/FM bilayers are two independent resistors (R_{FM} or R_{NM}) in parallel (see the inset to Fig. 4), which is known as the two-channels model. In this model, it is also assumed that the Hall voltage is only generated by the FM layer. Then, the total current I_t and voltage V_t along the sample can be expressed as $I_t = I_{FM} + I_{NM}$ and $V_t = R_{FM}I_{FM} = R_{NM}I_{NM}$, where the FM and NM subscripts indicate the FM and NM layer, respectively. Consequently, V_{AH} from the FM (= CoFeB) layer can be given by[16]

$$V_{AH} = \left(\frac{\rho_{AH}}{d_{CoFeB}}\right)\frac{I_t}{(R_{CoFeB}/R_{NM})+1} \approx \frac{1}{(R_{CoFeB}/R_{NM})+1}, \tag{9}$$

where d_{CoFeB} and ρ_{AH} are the thickness of CoFeB layer and the anomalous Hall resistivity in bilayer, respectively. Based on Eq. (9), the V_{AH} values of the Pt and Pd NM case are

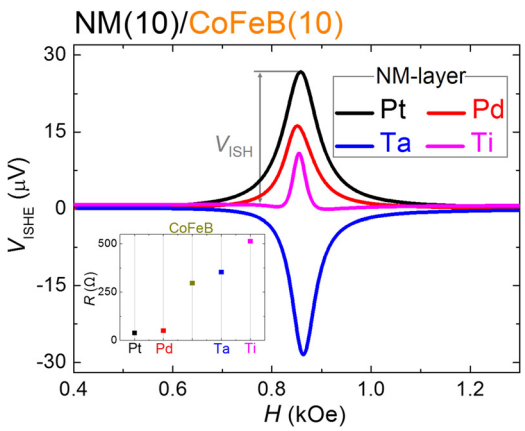

FIG. 3. The H dependence of V_{ISHE} based on Eq. (6). The inset shows the resistance of the single layer (1 mm × 2 mm) for Pt, Pd, CoFeB, Ta, and Ti.

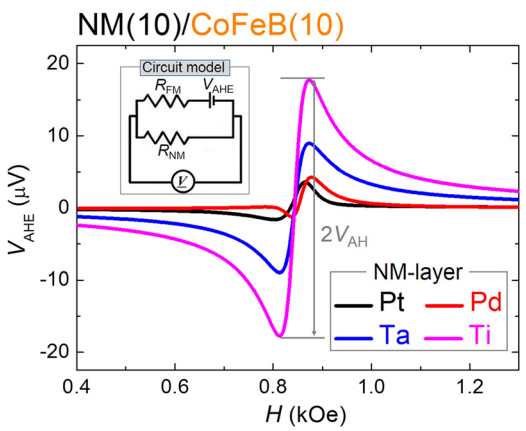

FIG. 4. The H dependence of V_{AHE} based on Eq. (8). The inset shows an equivalent circuit model for the AHE contribution.

smaller than that of Ta and Ti NM case. That is, the AHE contribution is significantly decreased for the $R_{FM}/R_{NM} > 1$ condition such as $R_{CoFeB}/R_{Pt} = 7.6$ and $R_{CoFeB}/R_{Pd} = 5.8$. On the contrary, the AHE contribution is fairly dominant for the $R_{FM}/R_{NM} < 1$ condition such as $R_{CoFeB}/R_{Ta} = 0.84$ and $R_{CoFeB}/R_{Ti} = 0.58$. In the bilayer system, it is important that the relative contributions between the ISHE and AHE depend on the R-ratio between the FM and NM layer. When only the ISHE term is considered in the bilayer, V_{ISHE} was previously written as a simple circuit model ($V_{ISHE} \propto R_{FM}R_{NM}/(R_{FM} + R_{NM})$). Highly resistive NMs were employed in the NM layer to obtain the large V_{ISH} value. However, according to the above results, it is unavoidable that NMs with large R values exhibit the unwanted AHE in bilayer samples.

IV. CONCLUSIONS

The dependence of the measured voltage on the NM in bilayer systems has been investigated under FMR conditions in the TE_{011} resonant cavity. The directional change of V_{ISHE} for the bilayer stacking order can separate the pure V_{ISHE} and V_{AHE} utilizing the method of addition and subtraction. Both Ta and Ti materials show the broad deviation of θ_{ISH}, which originates from the AHE in accordance with the high resistivity of NMs. However, both Pt and Pd materials show that the NMs with low resistivity are consistent with the previously reported θ_{ISH} values. Therefore, the characteristics of NM should be simultaneously satisfied with large θ_{ISH} and low resistivity to obtain reasonable and pure V_{ISHE} values in bilayer systems. These results will provide significant knowledge for designing high purity J_s-generators or detectors.

ACKNOWLEDGMENTS

This research was supported by the Pioneer Research Center Program through the National Research Foundation of Korea funded by the Ministry of Science, ICT & Future Planning (2011-0027908); by a grant from the R&D Program for Industrial Core Technology funded by the Ministry of Trade, Industry and Energy (MOTIE), Republic of Korea (Grant No. 10044723); by the KBSI Grant Nos. T34517 and T34437 for S.-Y.P.; and by National Research Foundation (Nos. NRF-2012R1A1A1041590 and NRF-2012K2A1A2033057) funded by the Ministry of Science, ICT & Future Planning.

[1]S. A. Wolf, D. D. Awschalom, R. A. Buhrman, J. M. Daughton, S. von Molnar, M. L. Roukes, A. Y. Chtchelkanova, and D. M. Treger, Science **294**, 1488 (2001).
[2]K. Uchida, M. Ishida, T. Kikkawa, A. Kirihara, T. Murakami, and E. Saitoh, J. Phys.: Condens. Matter **26**, 343202 (2014).
[3]F. J. Jedema, A. T. Filip, and B. J. van Wees, Nature (London) **410**, 345 (2001).
[4]E. Saitoh, M. Ueda, H. Miyajima, and G. Tatara, Appl. Phys. Lett. **88**, 182509 (2006).
[5]O. Mosendz, J. E. Pearson, F. Y. Fradin, G. E. W. Bauer, S. D. Bader, and A. Hoffmann, Phys. Rev. Lett. **104**, 046601 (2010).
[6]K. Ando, S. Takahashi, J. Ieda, H. Kurebayashi, T. Trypiniotis, C. H. W. Barnes, S. Maekawa, and E. Saitoh, Nat. Mater. **10**, 655 (2011).
[7]C. Hahn, G. de Loubens, O. Klein, M. Viret, V. V. Naletov, and J. Ben Youssef, Phys. Rev. B **87**, 174417 (2013).
[8]A. Hoffmann, IEEE Trans. Magn. **49**, 5172 (2013).
[9]K. Ando and E. Saitoh, J. Appl. Phys. **108**, 113925 (2010).
[10]Y. Tserkovnyak, A. Brataas, and G. E. W. Bauer, Phys. Rev. Lett. **88**, 117601 (2002).
[11]K. Ando, S. Takahashi, J. Ieda, Y. Kajiwara, H. Nakayama, T. Yoshino, K. Harii, Y. Fujikawa, M. Matsuo, S. Maekawa, and E. Saitoh, J. Appl. Phys. **109**, 103913 (2011).
[12]K. Harii, K. Ando, H. Y. Inoue, K. Sasage, and E. Saitoh, J. Appl. Phys. **103**, 07F311 (2008).
[13]S. Kim, M. Seo, and S. Park, J. Appl. Phys. **115**, 17C501 (2014).
[14]R. Takahashi, R. Iguchi, K. Ando, H. Nakayama, T. Yoshino, and E. Saitoh, J. Appl. Phys. **111**, 07C307 (2012).
[15]H. Nakayama, K. Ando, K. Harii, T. Yoshino, R. Takahashi, Y. Kajiwara, K. Uchida, Y. Fujikawa, and E. Saitoh, Phys. Rev. B **85**, 144408 (2012).
[16]W. J. Xu, B. Zhang, Z. Wang, S. S. Chu, W. Li, Z. B. Wu, R. H. Yu, and X. X. Zhang, Eur. Phys. J. B **65**, 233 (2008).